

Chemical transformation and morphology change of nickel–silica hybrid nanostructures *via* nickel phyllosilicates†

Ji Chan Park,^a Hyun Ju Lee,^b Jung Up Bang,^a Kang Hyun Park^{*b} and Hyunjoon Song^{*a}

Received (in Cambridge, UK) 14th August 2009, Accepted 14th October 2009

First published as an Advance Article on the web 26th October 2009

DOI: 10.1039/b916837k

Ni@SiO₂ core-shell nanoparticles were transformed to Ni particles on silica spheres *via* a branched nickel phyllosilicate phase by hydrothermal and hydrogen reduction reactions; the final morphology was successfully employed as an active nanocatalyst for the hydrogen transfer reaction of acetophenone.

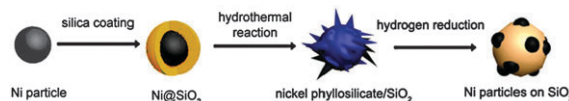
As particle size decreases, physical and chemical properties of materials are largely dominated by their surface nature.¹ In general, chemical reactions of nanostructured materials proceed more rapidly than those of the bulk forms, because of large surface-to-volume ratio and high surface energy. As well as such enhanced reactivity, chemical transformation usually accompanies simultaneous morphological change of the original structure. For instance, oxidation of cobalt nanoparticles in solution converts their shapes from spherical to porous hollow shells through the nanoscale Kirkendall effect.² This morphology change directly adjusts the material properties, and can open up a wide range of applications.

Recently, metal–silica hybrid nanostructures have been investigated in various fields, such as catalysis, sensing, imaging, and therapy, due to silica's high thermal stability and biocompatibility with controllable pore textures, and because it does not alter the physical nature of the metal components.³ The inertness of the silica framework allows it to be a nanosized reaction vessel, where chemical reactions occur under a stable environment even at high temperature.⁴ In some cases, silica can participate in the reaction with metals to form metal phyllosilicates (or metal silicate hydroxides), which is important for stabilization of metal nanoparticles on the catalyst support.⁵

In the present work, we report on a novel chemical transformation and subsequent morphology change of a nickel–silica hybrid system. Nickel cores inside silica shells in Ni@SiO₂ formed nickel phyllosilicate with an urchin-like morphology under hydrothermal conditions, and tiny nickel nanoparticles were regenerated on silica spheres by hydrogen reduction (Scheme 1). The resulting Ni/SiO₂ nanospheres showed high activity and reusability for the hydrogen transfer reaction of acetophenone.

Nickel nanoparticles were synthesized by thermal decomposition of nickel–oleylamine complexes.⁶ The nickel precursor, nickel(II) acetylacetonate, was dissolved in a mixture of oleylamine and trioctylphosphine (TOP). The resulting mixture was slowly heated to 230 °C for 20 min, and aged for 40 min at the same temperature. The transmission electron microscopy (TEM) image shows monodisperse nickel nanoparticles with an average diameter of 5.3 ± 0.2 nm (Fig. 1a). The high resolution TEM (HRTEM) image of a single nanoparticle exhibits continuous atomic lattice fringes (Fig. 1b), indicating its single-crystallinity. The distance between neighbouring fringe images is 0.20 nm, corresponding to the lattice spacing of (111) crystallographic planes. The X-ray diffraction (XRD) pattern represents a face-centered cubic (fcc) nickel structure (JCPDS No. 04-0850), and the electron diffraction (ED) shows two ring patterns, assignable to (111) and (220), respectively (Fig. S1, ESI†). The nickel nanoparticles were successfully coated with silica using the microemulsion method.⁷ A nickel particle dispersion in cyclohexane was mixed with Igepal CO-630 and ammonia, and tetramethyl orthosilicate (TMOS) was simultaneously injected into the mixture, which was stirred at room temperature for 1 h. The TEM images show that silica layers are uniformly coated outside the nickel cores with an average thickness of 9.2 ± 1.1 nm (Fig. 1c and d). More than 90% of the silica spheres contain single nickel cores. The average diameter of the Ni@SiO₂ particles is estimated to be 26 ± 2 nm. The XRD pattern is a simple combination of an intense peak of SiO₂ and small peaks of fcc nickel.

The Ni@SiO₂ core-shell particles are stable under neutral conditions. However, when the particle dispersion in water was refluxed under weak basic conditions (pH = 9.6), the black dispersion turned dark green within 20 min. The TEM image shows spherical particles having needle-like, thin branches (Fig. 2a). The average diameter of the spheres is estimated to be 25 ± 1 nm, which is unchanged from the original Ni@SiO₂ diameters. The branches are *ca.* 5 nm in length and 1 nm in thickness, dimensions typically observed in the nickel phyllosilicate phase. The XRD peaks are discernable at $\theta = 34, 37, \text{ and } 61^\circ$, and are clearly assigned to (200), (202), and (060) diffractions of pectoraite Ni₃Si₂O₅(OH)₄ (JCPDS No. 49-1859), respectively. The broad



Scheme 1 Chemical transformation and subsequent morphology change of nickel–silica hybrid nanoparticles.

^a Department of Chemistry, Korea Advanced Institute of Science and Technology, Daejeon, 305-701, Korea. E-mail: hsong@kaist.ac.kr; Fax: +82-42-350-2810; Tel: +82-42-350-2847

^b Department of Chemistry, Pusan National University, Busan, 609-735, Korea. E-mail: chemistry@pusan.ac.kr; Fax: +82-51-980-5200; Tel: +82-51-510-2238

† Electronic supplementary information (ESI) available: Details of experimental procedures, XRD spectra, N₂ sorption isotherms, and TEM and HRTEM images of the products, and ¹H-NMR spectra of the reactants and products in hydrogen transfer reactions. See DOI: 10.1039/b916837k

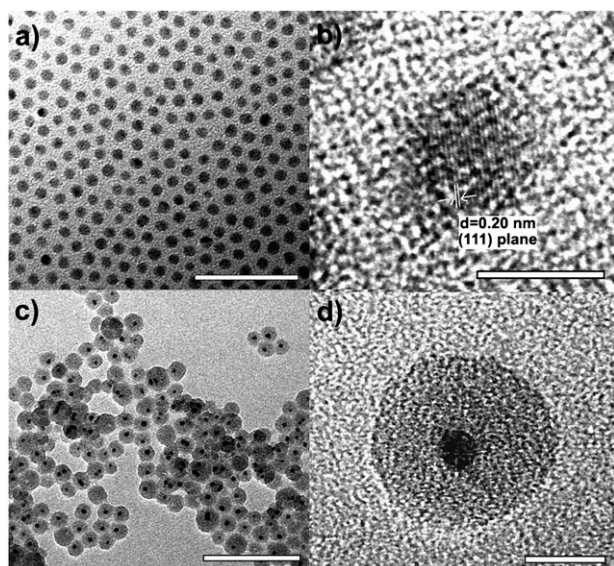


Fig. 1 TEM and HRTEM images of (a,b) Ni and (c,d) Ni@SiO₂ nanoparticles. The bars represent (a) 50 nm, (b) 5 nm, (c) 100 nm, and (d) 10 nm.

peaks centered at $\theta = 21\text{--}24^\circ$ correspond to the overlap of residual amorphous SiO₂ and (004) of nickel phyllosilicate. These results indicate that the particles are composed of the main silica spheres and nickel phyllosilicate branches.

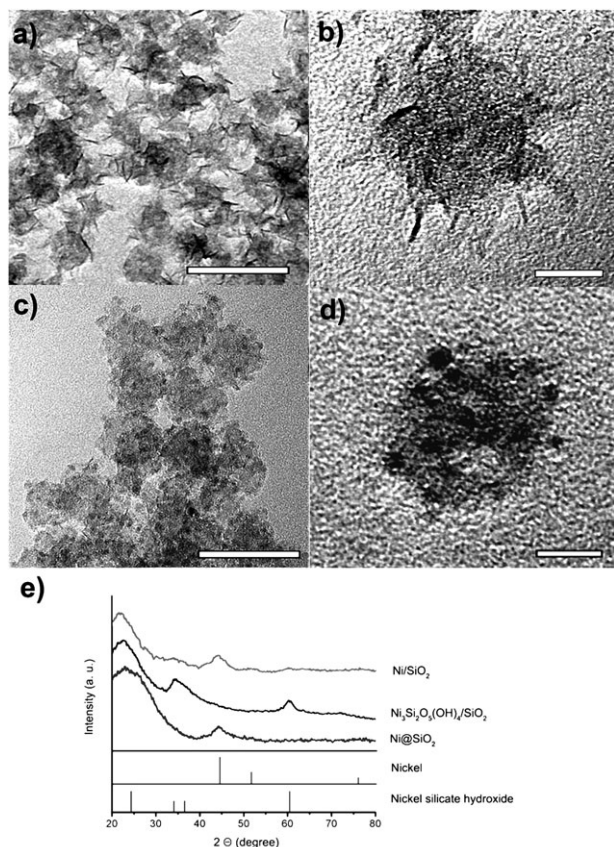


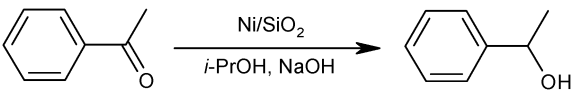
Fig. 2 TEM and HRTEM images of (a,b) nickel phyllosilicate/SiO₂ and (c,d) Ni/SiO₂ nanostructures. (e) XRD spectra of Ni@SiO₂, nickel phyllosilicate/SiO₂, and Ni/SiO₂ nanostructures. The bars represent (a,c) 50 nm and (b,d) 10 nm.

Nickel phyllosilicates are generally prepared through precipitation of nickel onto a silica surface by basification of nickel(II) solutions under a hydrothermal condition.⁸ In a basic solution, nickel hydroxide is the most thermodynamically stable species among nickel aqua species at a temperature range of 25–100 °C, according to the Pourbaix diagram.⁹ The nickel hydroxide species react with silicic acid to form Ni–O–Si bonds, and subsequent steps of polymerization lead to the layered structure of nickel phyllosilicate. Burattin *et al.* suggested the formation nickel phyllosilicates on silica matrix both by Ni–O–Si hetero-condensation/polymerization and by Ni–OH–Ni ololation/polymerization routes.¹⁰ Cui *et al.* also reported branched nickel phyllosilicates generated by the dissolution of a nickel salt and the simultaneous condensation with silica.^{5b} Based on these mechanisms, the formation process of the branched spheres from the Ni@SiO₂ nanoparticles is proposed as follows. (i) The nickel(0) cores are oxidized to form nickel hydroxides under a hydrothermal condition. (ii) Nickel hydroxide species are diffused into the silica layers through defects and pores, and react with the surface hydroxides on the walls to yield 1:1 nickel phyllosilicate. (iii) Further polymerization occurs on the Ni(II) sites, thereby extending thin branches outward from the original silica shells.

This urchin-like morphology with the thin branches provides a high surface area of the constituent materials. A nitrogen sorption experiment result at 77 K exhibits a type-IV isotherm with type H3 hysteresis (Fig. S2, ESI†). The surface area and pore volume were estimated to be 388.5 m² g⁻¹ and 0.95 cm³ g⁻¹, respectively, comparable to those of mesoporous silica balls.

The thin branches were easily deformed and converted to dark dots when the electron beam was directly irradiated during the TEM measurement (Fig. S3, ESI†). The high energy electrons may reduce the nickel phyllosilicate to form nickel nanoparticles. It is known that high temperature treatment of nickel phyllosilicate leads to dehydroxylation of silicate and nickel oxide formation.¹¹ Motivated by the TEM result, the branched nickel phyllosilicate particles were treated at 700 °C for 10 h under a continuous hydrogen flow. Sufficient reduction yielded amorphous silica and fcc nickel peaks in the XRD spectrum (Fig. 2e). The TEM image clearly shows the morphology change of the Ni/SiO₂ nanoparticles (Fig. 2c and d), where tiny nickel nanoparticles are located on the surface of silica spheres. The average diameter of the silica spheres is 24 ± 1 nm, which is nearly identical to the diameter of the original Ni@SiO₂ and branched nickel phyllosilicate nanoparticles. The tiny nickel particles are single crystalline, and the mean diameter is ~3 nm, as measured from the HRTEM image (Fig. S4, ESI†). This is in good agreement with the value (2.5 nm) calculated from the FWHM of the (111) peak in the XRD spectrum using the Debye–Scherrer equation. The lattice spacing between neighboring fringes is 0.20 nm, corresponding to that of (111) in fcc nickel. The Ni loading content is measured to be 30 wt% by energy dispersive X-ray fluorescence (EDXRF) spectroscopy. The surface area and total pore volume of the particles are calculated to be 220 m² g⁻¹ and 0.69 cm³ g⁻¹ (Fig. S2, ESI†), respectively, reflecting morphology change from branches to tiny nanoparticles on the silica spheres.

Table 1 Hydrogenation transfer of acetophenone to 1-phenylethanol catalyzed by Ni(30 wt%)/SiO₂ nanocatalyst



Entry	Cat (mol%)	T/°C	Time/h	Conv. (%) ^a
1	0.01	100	1	79
2	0.05	100	1	93
3	0.1	150	1	97
4	0.1	100	1	94
5	0.1	80	1	54
6	0.1	100	0.5	88
7	Recovered from #2	100	1	93
8	Recovered from #7	100	1	97
9	Recovered from #8	100	1	90
10	Recovered from #9	100	1	92

^a Determined by ¹H-NMR spectra. Yields are based on the amount of acetophenone used.

It is interesting that the nickel atoms concentrated on the center of the Ni@SiO₂ particles were evenly distributed in the silica matrix as a form of nickel phyllosilicate, and eventually migrated to the silica surface, generating tiny nickel particles. The final morphology of the Ni/SiO₂ nanostructure can be regarded as active metal nanoparticles embedded on the silica support, and thereby it is a promising bifunctional catalyst for various heterogeneous reactions. It is worth noting that apparent sintering of the nickel nanoparticles was not observed during heat treatment at 700 °C for 10 h, although the particle size is only ~3 nm. This high thermal stability is attributed to strong chemical interaction between the nickel particles and the silica surface through Ni–O–Si bonding, which originates from the nickel phyllosilicate phase.

Catalytic activity of the Ni/SiO₂ nanoparticles was examined for the hydrogen transfer reaction of acetophenone. The heterogeneous hydrogen transfer reaction is known to be superior to other reduction methods of organic compounds, because of its simple reaction process and reusability.¹² The reactions were carried out with isopropanol as a hydrogen donor at 80–150 °C (Table 1). When 0.05 mol% of the catalyst was used with respect to the substrate amount, acetophenone was successfully converted to 1-phenylethanol at 100 °C within 1 h in 93% yield (entry 2) without any by-products. To the best of our knowledge, the Ni/SiO₂ nanoparticles exhibit the highest catalytic activity among heterogeneous nickel catalysts for hydrogen transfer reactions,¹³ in that most of the previous reactions used 10–50 mol% of the nickel catalysts to obtain high yields of the products.¹⁴ This remarkably high activity is attributed to the small particle size (~3 nm) and even dispersion of the active nickel nanoparticles on the silica support. The conversion rates were affected by the reaction

time and temperature (entries 3–6). After the reaction, the Ni/SiO₂ nanocatalysts were readily separated by centrifugation and could be reused five times under the present reaction conditions without any loss of catalytic activity (entries 7–10, Fig. S6, ESI†).

In conclusion, we have synthesized a Ni/SiO₂ nanocatalyst bearing tiny nickel nanoparticles embedded on silica spheres by chemical transformation of Ni@SiO₂ core-shells through the branched nickel phyllosilicate phase. The final morphology behaves as a highly active nanocatalyst for the hydrogen transfer reactions. It is anticipated that this approach can be a potential synthetic method for other bifunctional catalytic systems forming metal phyllosilicates, such as cobalt and magnesium/silica nanostructures.

This work is dedicated to Prof. Joon T. Park on the occasion of his 60th birthday, and was supported by the Pioneer Research Program from the Korea Science and Engineering Foundation (KOSEF) under contract No. 2008–05103. This research was also supported by the Basic Science Research Program through the National Research Foundation of Korea (NRF) funded by the Ministry of Education, Science and Technology (2009–0070926).

Notes and references

- (a) G. A. Somorjai, *Introduction to Surface Chemistry and Catalysis*, John Wiley and Sons, Inc., 1994; (b) G. Cao, *Nanostructures & Nanomaterials. Synthesis, Properties & Applications*, Imperial College Press, 2004.
- Y. Yin, R. M. Rioux, C. K. Erdonmez, S. Hughes, G. A. Somorjai and A. P. Alivisatos, *Science*, 2004, **304**, 711.
- (a) J. Lee, J. C. Park and H. Song, *Adv. Mater.*, 2008, **20**, 1523; (b) S. Liu and M. Han, *Adv. Funct. Mater.*, 2005, **15**, 961; (c) Y. Deng, D. Qi, C. Deng, X. Zhang and D. Zhao, *J. Am. Chem. Soc.*, 2008, **130**, 28.
- S. H. Joo, J. Y. Park, C.-K. Tsung, Y. Yamada, P. Yang and G. A. Somorjai, *Nat. Mater.*, 2009, **8**, 126.
- (a) P. Jin, Q. Chen, L. Hao, R. Tian, L. Zhang and L. Wang, *J. Phys. Chem. B*, 2004, **108**, 6311; (b) Z. Guo, F. Du, G. Li and Z. Cui, *Chem. Commun.*, 2008, 2911.
- J. Park, E. Kang, S. U. Son, H. M. Park, M. K. Lee, J. Kim, K. W. Kim, H.-J. Noh, J.-H. Park, C. J. Bae, J.-G. Park and T. Hyeon, *Adv. Mater.*, 2005, **17**, 429.
- D. K. Yi, S. T. Selvan, S. S. Lee, G. C. Papaefthymiou, D. Kundaliya and J. Y. Ying, *J. Am. Chem. Soc.*, 2005, **127**, 4990.
- A. McDonald, B. Scott and G. Villemure, *Microporous Mesoporous Mater.*, 2009, **120**, 263.
- B. Beverskog and I. Puigdomenech, *Corros. Sci.*, 1997, **39**, 969.
- (a) P. Burattin, M. Che and C. Louis, *J. Phys. Chem. B*, 1998, **102**, 2722; (b) T. Mizutani, Y. Fukushima, A. Okada and O. Kamigaito, *Bull. Chem. Soc. Jpn.*, 1990, **63**, 2094.
- P. Burattin, M. Che and C. Louis, *J. Phys. Chem. B*, 2000, **104**, 10482.
- R. A. W. Johnstone and A. H. Wilby, *Chem. Rev.*, 1985, **85**, 129.
- (a) M. Kidwai, N. K. Mishra, V. Bansal, A. Kumar and S. Mozumdar, *Catal. Commun.*, 2008, **9**, 612; (b) F. Alonso, P. Riente and M. Yus, *Synlett*, 2008, 1289; (c) F. Alonso, P. Riente and M. Yus, *Eur. J. Org. Chem.*, 2008, 4908.
- (a) F. Alonso, P. Riente and M. Yus, *Tetrahedron Lett.*, 2008, **49**, 1939; (b) F. Alonso, P. Riente and M. Yus, *Tetrahedron*, 2008, **64**, 1847.